ELASTIC ANALYSIS OF THRUST BEARINGS

Villar, M. M.
Faculdade de Engenharia Mecânica, Universidade Federal de Uberlândia, Brazil
mmvillar@mecanica.ufu.br

Pérez, M. M.
Faculdade de Engenharia Mecânica, Universidade Federal de Uberlândia, Brazil
marioperez@nanet.com.br

Abstract: The increase in the bearing loading and the drive for reducing dimensions and component masses in modern combustion engines have led to substantial elastic distortion in connecting-rod and main crankshaft bearings. This distortion, in turn, may seriously affect lubrication between journal and bearing surfaces. In such applications, the conventional bearing theories, which are based on the assumption of perfectly rigid journal and bearings, fail to provide answers to the problem and the coupling of hydrodynamic lubrication with the structural elasticity of the bearing – *i.e. an elasto-hydrodynamic analysis* – must be sought. The theory of elasto-hydrodynamic (EHD) lubrication allows to take the important effects of elastic deformation and pressure-dependent viscosity into consideration in bearing analysis. In this paper the Finite Element Method is used in order to simulate the behaviour of thrust bearing pads and achieve the pressure distribution acting on the surface of an elastic bearing as well as stress distribution.

Key words: elasto-hydrodynamic analysis, thrust bearing, finite element method, pressure distribution, stress analysis.

1. Introduction

Due to the increase in the bearing loading and the presence of lighter components some modern engines experience problems on their connecting-rod cap bearings. There is evidence that some bearings suffer severe wear while others were damaged by both wear and fatigue of the bearing lining when they are operated at high speeds, probably due to the deformation of the inserts and housings (Xu and Crooks, 1997). In such applications, the conventional bearing theory, which is based on the assumption of perfectly rigid bodies, fail to provide answers to the problem and the coupling of hydrodynamic lubrication with the structural analysis – *i.e. an elasto-hydrodynamic analysis* – must be sought. The theory of elasto-hydrodynamic (EHD) lubrication allows to take the important effect of elastic deformation into consideration in bearing analysis.

Pinkus and Sternlicht (1961) stated that, depending on bearing stiffness and assembly, the deformation on real bearings will produce a different film shape, with a drastic change in bearing performance. More recently Xu (1997) stated that the assumption of perfectly rigid housings may result in a computed maximum film pressure five times larger than the actual one, thus making clear the importance of considering the bearing elastic behaviour in stress analyses. It is also important to recall that the pressure distribution in the oil-film and the extension of the bearing zone are also affected by the characteristics of the oil.

To predict the behaviour of any engineering system the analyst has to refer to physical modelling or mathematical methods. In the finite element approach the domain is discretized into a number of subregions which are denominated finite elements. These elements are considered interconnected at nodal points located at the border of the subregions (elements). Trial functions (Burnett, 1987) over each element, usually polynomials, approximate the solution at any point as a function of the nodal values. With a sufficiently refined mesh, the assembly of the individual elements can represent a very high order solution over the complete region.

In order to simulate the behaviour of thrust bearings, a two-dimensional, infinitely long, elasto-hydrodynamic model of the bearing is adopted (Villar, 2003).Due to the very small oil film thickness, usually of the order of a few microns, the solution of the elasto-hydrodynamic problem can only be achieved numerically, by using extremely refined meshes (Boedo, 2002), and high performance computers (Xu, 1997).

The basic equations from which the theory of hydrodynamic lubrication is derived are the equations of conservation of momentum and the equation of conservation of mass (continuity equation). These two equations, along with a energy conservation equation, form a complete set of equations known as the Navier-Stokes equations. When this theory was first derived, by Osborne Reynolds, in 1886, it was assumed that bearing and journals, were perfectly rigid. However, perfectly rigid bodies do not exist in nature, and some deformation always takes place under load.

Possibly the most important assumption made by Reynolds was that the film thickness were so thin when compared to the bearing radius that all effects due to curvature of the fluid film could be neglected. This enabled him to replace a curved bearing with a flat bearing, called plane slider bearing (Shigley, 1972), and use a cartesian frame of reference.

2. Plane slider bearing

Plane slider bearings are actually found in fixed-pad thrust bearings, as shown in Fig. (2.1). These bearings consist essentially of a runner sliding over a plane fixed-pad, Fig. (2.2). The lubricant is brought into radial grooves and pumped into the wedge-shaped space by the motion of the runner. Thick-film, or hydrodynamic, lubrication is obtained if the speed of the runner is continuous and sufficiently high, if the lubricant has adequate viscosity, and if it is supplied in sufficient quantity. Figure (2.2) also provides a picture of the pressure distribution for perfectly rigid plane thrust bearings under conditions of thick-film lubrication.
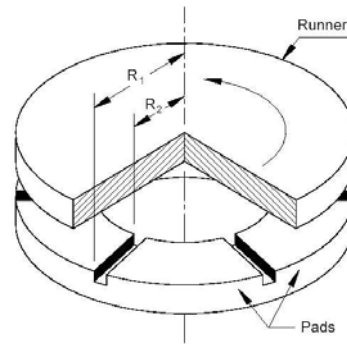
Figure 2.1. Fixed-pad thrust bearing (Shigley, 1972).
.
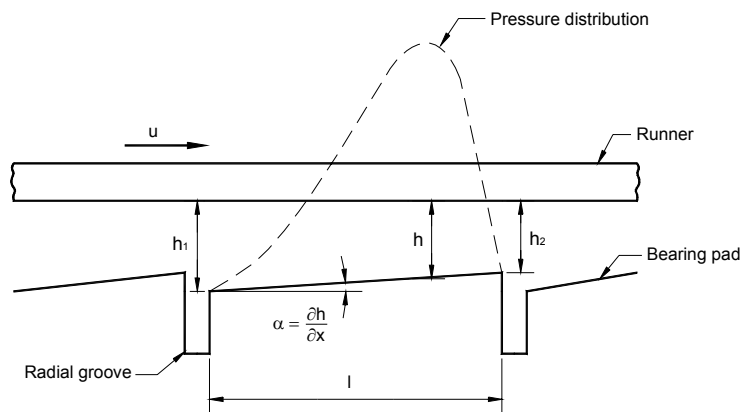
Figure 2.2. Lubricant pressure distribution in a perfectly-rigid plane thrust bearing pad.

The film thickness h in sectional segments of plane thrust bearings, Fig (2.2), can be expressed by

$$h = h_1 + \left(h_2 - h_1\right)\frac{x}{l}$$ (1)

where l is the length of the bearing pad.

2.1. Governing equations

For perfectly rigid, aligned bearings, the Reynolds equation, as shown in Eq. (2), is used to represent the behaviour of the fluid. The flow is considered as being incompressible, or rather, slow (creeping) fully incompressible (Pinkus and Sternlicht, 1961). In Eq.(2) u is the speed of the runner element .

$$\frac{\partial}{\partial h}\left(\frac{h^3}{\mu}\frac{\partial p}{\partial x}\right) + \frac{\partial}{\partial z}\left(\frac{h^3}{\mu}\frac{\partial p}{\partial z}\right) = 6u\frac{\partial h}{\partial x}$$ (2)

In the general form of the Reynolds equation, Eq. (2), the second term on the left-hand side is associated with side-leakage, or flow in the z – direction. In many conventional lubrication problems, side leakage can be neglected and the bearing can be assumed to be infinitely long.

If the side-leakage is neglected, Eq. (2) reduces to

$$\frac{d}{dh}\left(\frac{h^3}{\mu}\frac{dp}{dx}\right) = 6u\frac{dh}{dx} \tag{3}$$

which is the classical Reynolds equation for one-dimensional (x-direction) flow.

2.2. Boundary conditions

One of the major difficulties in obtaining satisfactory solutions for bearings lies in defining accurately the boundary conditions for the fluid film. Viscous flows depend strongly upon their boundary conditions (White, 1991). Boundary conditions for the fluid flow problem are the velocity at the solid boundaries (the no-slip condition) and the pressure at the points where it could be prescribed.

The lubricant can be admitted to a bearing at any point, and the deeper this point lies in the converging film the more pronounced is the effect on the resulting pressure distribution. As the lubricant is not always admitted at ambient or atmospheric (zero) pressure, a prescribed inlet pressure $p = \bar{p}$ is imposed either at the point where the lubricant enters the bearing, or at the beginning of the hydrodynamic pressure distribution.

2.3. Analytical solution for perfectly rigid infinitely long bearings

In the solution of the plane slider bearing it is considered that the slider (runner) moves at velocity u and creates a combined Couette-Poiseuille flow in the very narrow gap, Fig. (2.2) (White, 1991). The gap decreases from h_1 in the entrance to h_2 at the exit. The closed form solution to the hydrodynamic pressure distribution in a perfectly rigid linearly contracting gap with no vertical velocity is expressed by (White, 1991)

$$\frac{p - p_a}{\mu\,u\,l/h_1^2} = \frac{6\,(x-l)\,(1-x/l)\,(1-h_2/h_1)}{(1+h_2/h_1)\left[1-(1-h_2/h_1)\,x/l^2\right]} \tag{4}$$

where h is given by Eq. (1), μ is the viscosity, l is length of the bearing pad, and p_a is the pressure at the beginning and at the end of the bearing pad, i.e., $p_1 = p_2 = p_a$. .

2.4. Elasto-hydrodynamic lubrication

The high degree of geometrical and elastic conformity between the runner and the bearing pad enables substantial loads to be carried by relatively small oil film pressures, thus making it possible to assume the influence of the pressure on the viscosity of the lubricant negligible. Nevertheless, the loads transmitted by the fluid film can lead to substantial deformation of the bearing pad and the runner; an effect which can drastically change the geometry of the film. Since the shape of the film determines the pressure distribution, it is at once apparent that the solution to the elasto-hydrodynamic problem must simultaneously satisfy the governing equation of lubrication and the equations of elasticity. In the solution of elasto-hydrodynamic problems it has been found useful to solve the inverse problem; that is, to determine the shape of the lubricant film which will generate a given pressure distribution.

Many simplifying assumptions have to be made in order to make the elasto-hydrodynamic lubrication amenable to analytical and numerical treatment, either because of incomplete knowledge or because or mathematical difficulties. Assumptions such as isoviscous flow - where the viscosity remains constant, smooth surface, static loading, incompressible, isothermal and laminar flow may, however, lead to a rather poor approximation.

3. Finite element modelling

During the last two decades much progress has been made toward the analysis of the general fluid flow problems using finite element procedures, and at present very complex fluid flows are solved (Bathe, 1996; Zienkiewicz and Taylor, 1991). Ansys 5.7® is used to simulate the behaviour of the flow and the fluid-structure interaction.

In elasto-hydrodynamic analyses neither the fluid behaviour nor the structural equations can be solved independently as the structural motions influence and react with the generation of pressures. Here interaction is significant and coupling occurs on the interfaces with runner and bearing pad. On the solid boundaries the velocities can be prescribed and the fluid-structure coupling may be described by computing the displacement due to a previously computed pressure distribution. Once the first solution of the fluid problem is obtained, usually for a perfectly rigid system, the pressure distributions at the runner and bearing interfaces are substituted for the solution of the structural problem, allowing its independent treatment. The computed displacements at the interfaces are then used to proceed in a *staggered* (Zienkiewicz and Taylor, 1991), *separated* (Brebbia, 1987), *weak or sequential* (ANSYS, 2002) fashion between fluid and structural solutions, until convergence is achieved.

3.1. Mesh-evolution strategy

A mesh-evolution strategy is a set of rules by which meshes are redesigned to arrive at an acceptable mesh. To estimate the accuracy and efficiency associated with the first (coarse) mesh and the criteria for mesh redesign, the results obtained are compared to the analytical solution to the problems of perfectly rigid bearings (Villar, 2003). It is assumed that the finite element approximation to the solution of the elasto-hydrodynamic problem will yield the exact solution to the mathematically posed problem in the limit, as the size h of elements decrease. The influence of the mesh on the numerical accuracy is tested by comparing results obtained by grid-size variation to results obtained by using the analytical solutions available in the literature for perfectly rigid slipper-pad.

A sequence of simple regular grids based on the reduction of the grid interval by halving the mesh size is adopted. The purpose of this approach is to achieve a monotonically convergent sequence of results (Melosh and Utku, 1987). This procedure ensures that each mesh includes the model of its predecessor as a subset. In regular meshes every element is of the same type and shape, but not of the same size. Richardson's extrapolation technique is used to find the value of the response corresponding to zero mesh size. In addition to this, some experiments indicate that when more than two analyses are required to attain the desired accuracy, extrapolation makes regular meshes more efficient than development of the results by any mesh. The conclusion is valid even if the 'wrong' element has been chosen to attain the accuracy desired. This is indeed the present case due to the fact that no quadratic element type is available for fluid modelling when ANSYS 5.7 fluid-structure interaction analysis is used.

Richardson's extrapolation is used to improve the results obtained by using the finite element method. From the solutions obtained by using interpolation functions of order $O(h^p)$ it is possible to get an approximation to the exact solution of order $O(h^{p+1})$. Thus, for instance, if we have to approximate solutions $u(h)$ and $u(h/2)$ obtained with meshes of size h and $h/2$, the Richardson's extrapolation value for u is defined as:

$$u_R(h) = \frac{2^P u(h/2) - u(h)}{(2^P - 1)} \tag{5}$$

Another use of this technique is to get an estimate of the error in the original approximation $u(h)$ or $u(h/2)$. This error should be approximately $u_R - u(h)$ or $u_R - u(h/2)$, respectively. Although one does not known how much more accurate approximation u_R is, to be conservative, one can always use $u_R - u(h)$ or $u_R - u(h/2)$ as an indication of the error (www.math.ubc.ca/~feldman/m256/richard.pdf, 2001).

For the cases where the analytical solution to the problem u is known (perfectly rigid bearings), the local error at node i, e_{li}, is defined as

$$e_{li} = u_i - u_{Ri} \tag{6}$$

For the definition of the global error e_g it is necessary to choose a norm in order to get some measure of the magnitude of the error at each node. The vector norm adopted is the discrete Euclidian (quadratic) norm π_E

$$\pi_E(e_{li}) = \| \mathbf{u} - \mathbf{u}_R \| = \sqrt{\sum_{i=1}^{n} (u_i - u_{Ri})^2} \tag{7}$$

where n is the number of nodal points considered. This leads to the definition of the global error as being

$$e_g = \pi_E(e_{li}) \tag{8}$$

while the relative error e_r is expressed by

$$e_g = \frac{e_g}{\pi_E(u_i)} \tag{9}$$

For the cases that do not have analytical solution it is necessary to compare the numeric results to the extrapolated values obtained by taking samples of the numerical results in the form shown in Fig. (3.1).
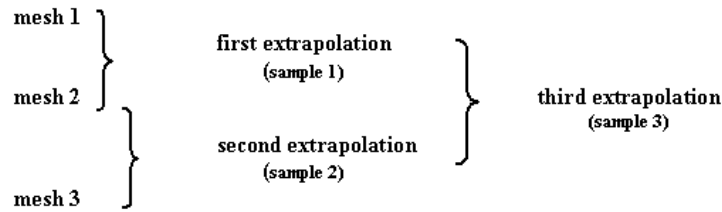
Figure (3.1). Sampling of results in order to get Richardson Extrapolation

3.2. Modelling description

The bearings analysed are assumed either as being perfectly rigid or as being constituted of elastic parts. The elastic bearings consist of a thin layer of an antifriction alloy perfectly bonded to a stiff backing that is supported either by a perfectly rigid or by an elastic support. The assumption that there is perfect bonding of the lining to the backing makes it possible to consider continuity of displacements in that region. For all models where the elasticity of the bearing part (bearing pad) and of the support are considered, it is assumed that there is no deformation in the direction perpendicular to the middle cross section of the bearing. The bearing is thus considered as being under a state of plane strain.

ANSYS$^{®}$ 5.7 Velocity-Thermo-Pressure coupled analysis with the *sequential* coupling method for fluid-structure interaction (ANSYS, 2002), is adopted in the present work. Computational Fluid Dynamics FLOTRAN and MULTIPHYSICS two-dimensional four-node isoparametric (linear) fluid-thermal FLUID141 and solid PLANE42 with extra displacement shapes (subparametric) are the finite element types used to build the models presented here. Fluid properties are regarded constant and it is assumed that the lining, the backing, and the support materials are linear elastic and isotropic.

Due to the fact that the ratio of the thickness of the fluid film to other dimensions of the bearing is very small, care is taken in order to keep the element aspect ratio (Desai and Abel, 1972) (ratio of the element larger side to the smaller) within acceptable limits in order to avoid degradation of the numerical solution. Consequently, as a fine mesh is needed to model the thickness of the fluid film, a fine mesh is also needed in the direction of the flow. This makes element sizes sufficiently small to keep the error approximation within acceptable bounds. The same is true with respect to the solid model due to the fact that the ratio of the thickness of the antifriction lining to other dimensions of the bearing is also very small.

The aspect ratio of the elements used to model the fluid film in the regions of steep pressure gradient in thrust bearings is *1 : 1*. This value is, however, conveniently augmented as one gets farther from those regions. Regular meshes are used whenever limitations on computer resources do not pose a problem to the numerical solution. When the available computer memory is insufficient to carry out the analysis, triangular unstructured meshes are used to connect elements with big differences in their aspect ratios. This procedure is adopted in order to limit the number of degrees of freedom of the model.

Three cases are modelled, which are Case 1 – Perfectly rigid thrust bearing pad; Case 2 – Elastic thrust bearing pad on a perfectly rigid support and Case 3 – Elastic thrust bearing pad on elastic support.

Case 1 - Perfectly rigid thrust bearing pad.

The initial mesh used for modelling the lubricant film in a perfectly rigid thrust bearing pad, Fig. (3.2), consists of 1024 × 3 FLUID141 elements. The initial mesh is refined to 2048 × 4 and to 4096 × 6 elements.
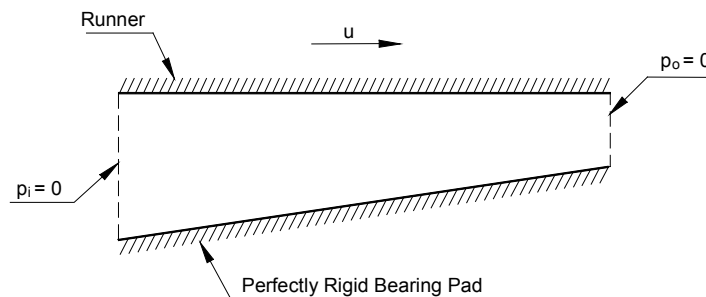
Figure (3.2) Configuration used for the analysis of the perfectly rigid thrust bearing pad.

Case 2 – Elastic thrust bearing pad on a perfectly rigid support.

The initial mesh used to model the coupling between the fluid with the elastic bearing pad consists of 1024×3 FLUID141 elements for the fluid, 1024×8 PLANE42 elements for the lining, and 1024×18 PLANE42 elements for the backing, Fig. (3.3). The initial mesh is then refined to 2048×4, 2048×12, and 2048×22, for the fluid, lining, and backing, respectively. Likewise, a third refinement is carried out to 4096×6, 4096×20, and 4096×36, for the fluid, lining, and backing, respectively.
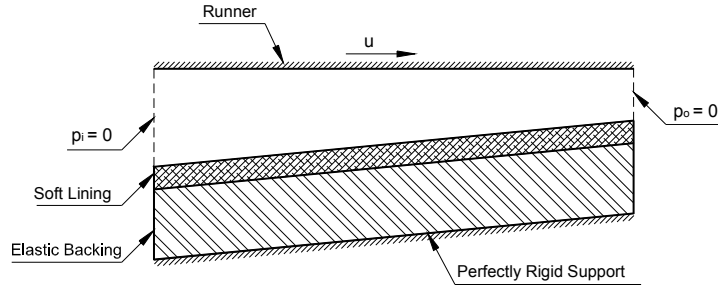
Figure (3.3). Configuration used for the analysis of the elastic thrust bearing pad on a rigid support.

Case 3 – Elastic thrust bearing pad on elastic support.

The elastic support is modelled by including a thick plate in the thrust bearing model, Fig. (3.4). Triangular PLANE42 elements are used in the model of the elastic backing in order to allow the use of uniform meshes (with aspect ratio $1 : 1$) in the elastic support.
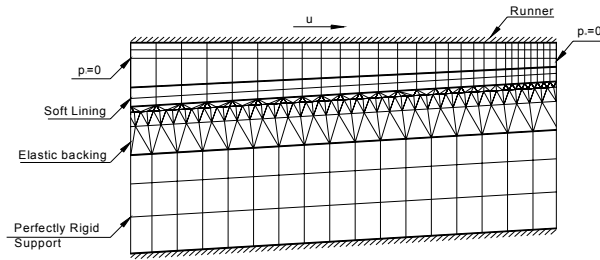
Figure (3.4). Schematic representation of the mesh configuration used for the analysis of the elastic thrust bearing pad on an elastic support.

4. Numerical results

Results of three mesh configurations and their extrapolated values are produced for the thrust bearing analyses. The elastic properties of the antifriction lining are assumed to be the material properties of the aluminium alloy AS124A. These are modulus of elasticity $E_l = 69.7$GPa, Poisson ratio $v_l = 0.33$, and compressive yield strength $Sy = 54.0$MPa (Joyce, 1999). The elastic properties of steel (modulus of elasticity $E_s = 207$GPa, and Poisson ratio $v_s = 0.29$) are taken for the backing and for the support.

Regarding the stress analysis, regions where tensile hoop stress occur at the surface of the bearing indicate where cracks are more likely to propagate. The peak of shear stress at the interface between the lining and the backing indicates the point within the lining where fatigue cracks are more likely to be nucleated.

The dimensions used for the thrust bearing models are length of the pad $l = 40.0$mm; entrance gap $h_0 = 0.1$mm; and exit gap $h_l = 0.03$mm (gap contraction ratio $h_l/h_0 = 0.3$), Fig. (3.2). The velocity of the runner is assumed to be $u = 10$m/s; while the viscosity $\mu = 0.625$Pa.s corresponds to the use of SAE 50 lubricating oil (White, 1991). It is assumed that the magnitude of the oil supply pressure is negligible compared to the generated pressures. In Case 1 the results for a perfectly rigid thrust bearing are presented. The elasticity of the bearing pad is considered in Case 2, Fig. (3.3), where the thickness of the aluminium lining is assumed to be $t_l = 0.25$mm, and thickness of the steel backing $t_b = 1.505$mm. A 12mm thick external plate is included in Case 3, where the influence of the elasticity of the bearing pad and the support is investigated.

Case 1 – Perfectly rigid thrust bearing

The pressure distribution obtained by implementing the analytical solution given by Eq.(4) is presented in Fig. (4.1a) and Fig.(4.1b), along with the pressure distributions obtained by using three different finite element mesh configurations. The results obtained by using Richardson extrapolation are presented in the Fig. (4.1b), while Tab (1), show the global error, and the relative error of the analysis.

(a)

(b)
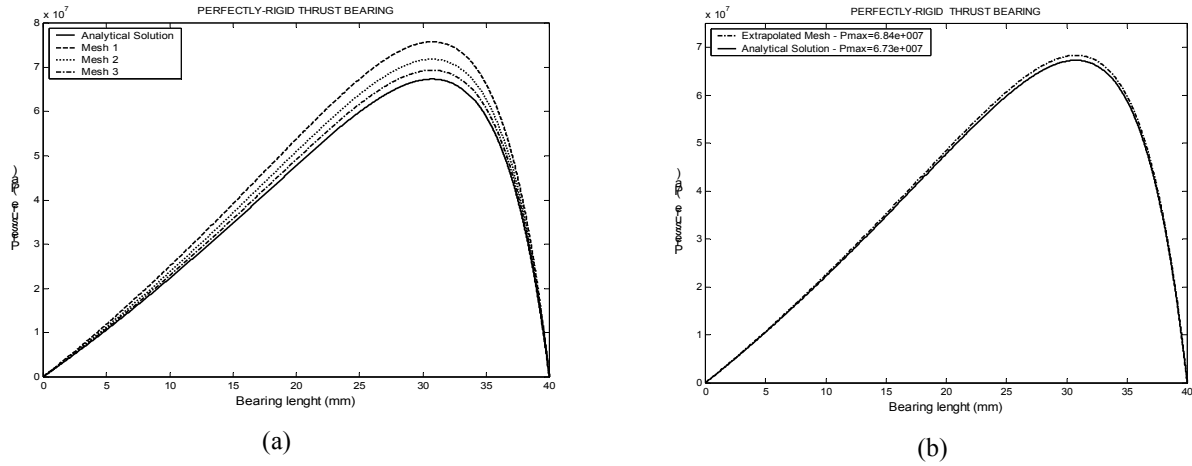
Figure (4.1). Pressure distribution for numerical results and extrapolated mesh – perfectly rigid thrust bearing

Table 1. Global error and relative error for the pressure distribution – perfectly rigid thrust bearing.

	Global error	Relative error
Sample 1	7.2102 e+07	4.75 %
Sample 2	3.8146 e+07	1.80 %
Sample 3	2.4032 e+07	1.60 %

Case 2 – Elastic thrust bearing pad on a perfectly rigid support.

The influence of the elasticity of the bearing pad on the hydrodynamic pressure distribution; of displacement and tangential stress at the surface of the bearing are presented in Figs (4.2) to (4.4), while Tab.(2) shows the global error and the relative error for the analysis, respectively. The distribution of shear stress within the lining at the interface with the backing is presented in Fig (4.3b). The results presented in Fig. (4.2b) allow to confirm that the elasticity of the support has a considerable influence on the pressure distribution.

(a)

(b)
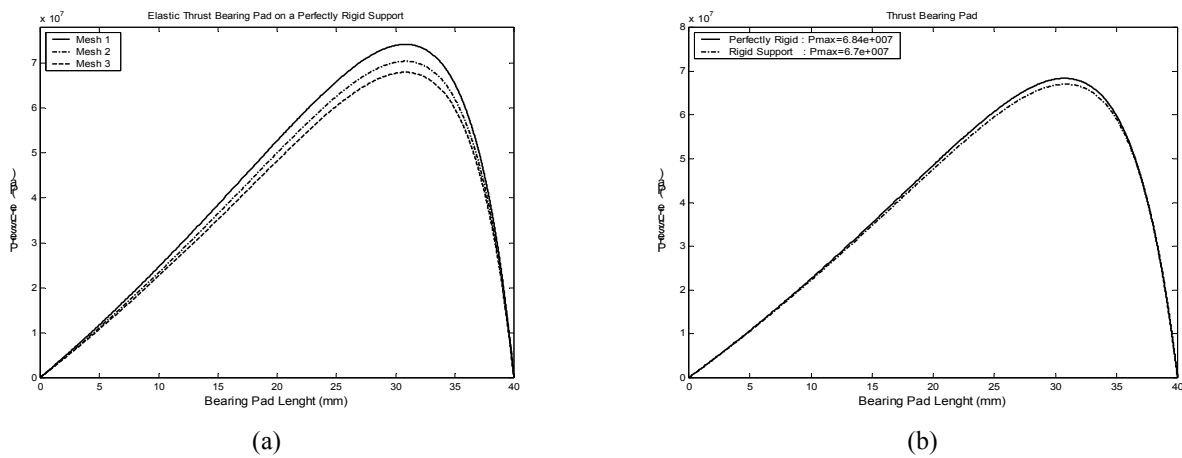
Figure (4.2). Pressure distribution on an elastic thrust bearing pad within perfectly rigid support (a) and pressure distribution on extrapolated mesh for elastic thrust bearing pad on perfectly rigid support in comparison with perfectly rigid thrust bearing (b).

Table 2. Global error and relative error for the pressure distribution – elastic thrust bearing pad on perfectly rigid support.

	Global error	Relative error
Sample 1	1.1498e+08	6.80 %
Sample 2	1.0640e+08	4.69 %
Sample 3	6.1986e+07	4.05 %

(a)

(b)
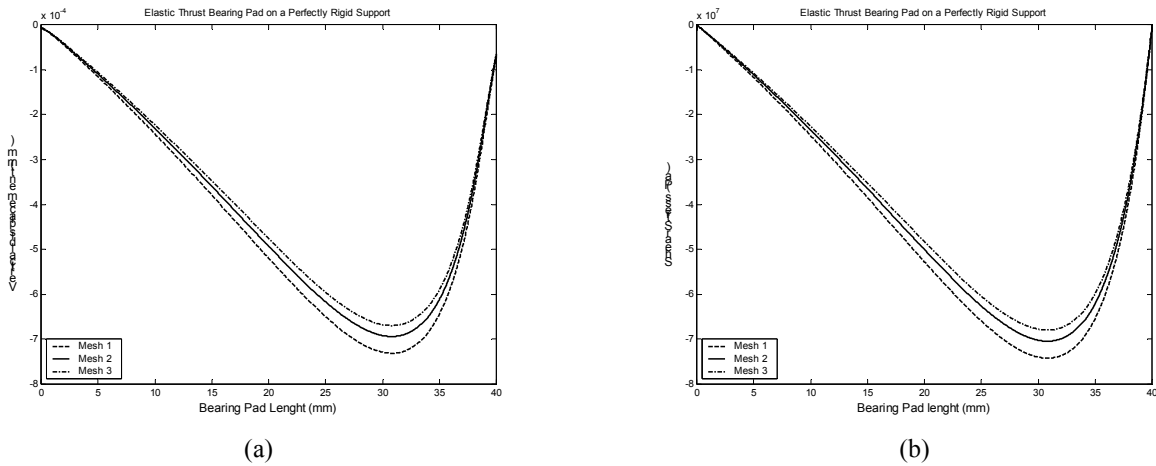
Figure (4.3). Distribution of vertical displacement at the bearing surface (a) and distribution of shear stress within the lining at the interface between the lining and the backing (b) - elastic thrust bearing pad on perfectly rigid support.
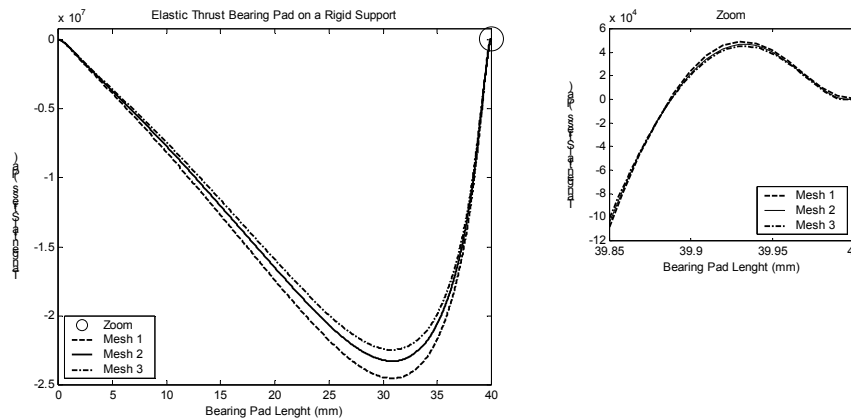
Figure (4.4). Distribution of the tangential stress at the bearing surface and the positive tangential stress region - elastic thrust bearing pad on perfectly rigid support.

Case 3 – Elastic thrust bearing pad on elastic support.

The influence of the elasticity of the bearing pad support on the hydrodynamic pressure distribution; on the distributions of vertical displacement and of tangential stress at the surface of the bearing are presented in Figs. (4.5) to (4.7), while Tab. (3) shows the global error and the relative error, respectively, of the analysis. The distribution of the shear stress within the lining at the interface with the backing is presented in Fig. (4.6b).

Table 3. Global error and relative error for the pressure distribution – elastic thrust bearing pad on elastic support.

	Global error	Relative error
Sample 1	9.0566e+07	6.10 %
Sample 2	8.3684e+07	4.17 %
Sample 3	4.8710e+07	3.58 %
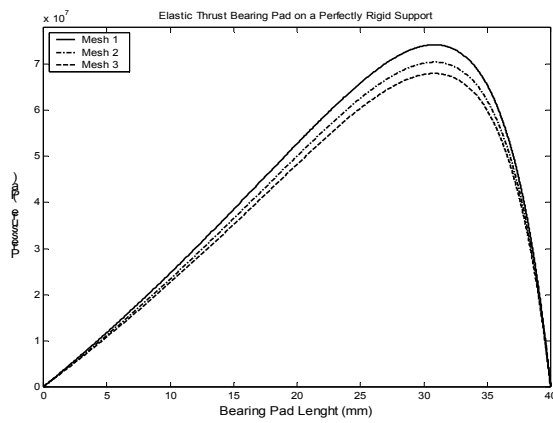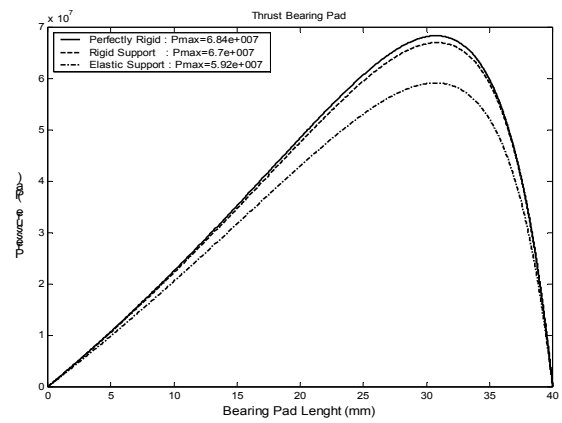
Figure (4.5). Pressure distribution on an elastic thrust bearing pad within elastic support (a) and pressure distribution on extrapolated mesh in comparison with perfectly rigid thrust bearing and perfectly rigid support (b).
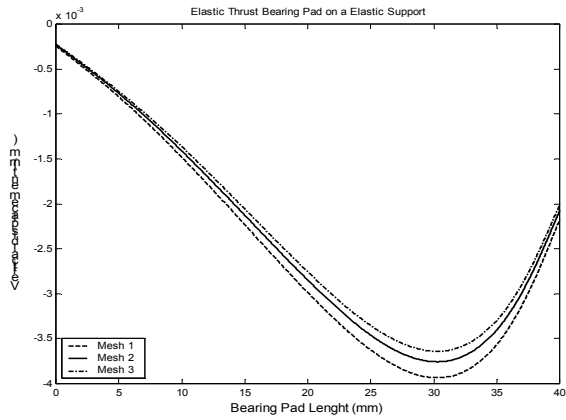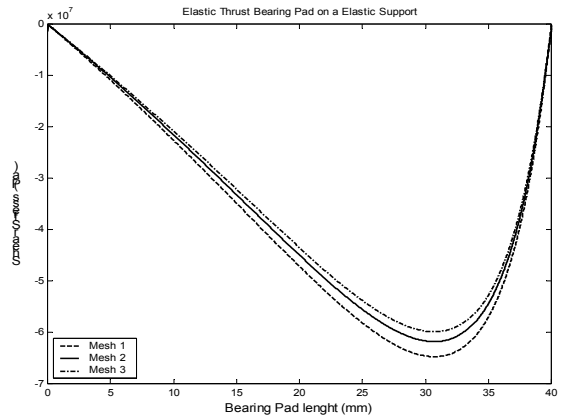
Figure (4.6). Distribution of vertical displacement at the bearing surface (a) and distribution of shear stress within the lining at the interface between the lining and the backing (b) - elastic thrust bearing pad on elastic support.
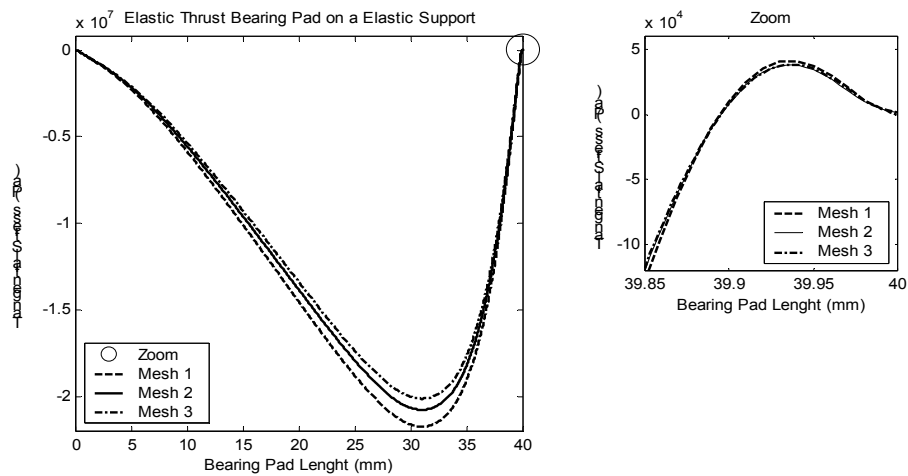
Figure (4.7). Distribution of the tangential stress at the bearing surface and the positive tangential stress region - elastic thrust bearing pad on elastic support.

4. Conclusions

Coupled fluid-structure two-dimensional finite element models are used to investigate the influence of the bearing elasticity on the hydrodynamic pressure distribution and on the stress distribution in the bearing. The elasticity of the housing is an important factor to consider if one wants to predict the life of the engine bearings with respect to fatigue. The results presented herein indicate that the pressure distribution in the lubricant is significantly affected by the elasticity of the bearing.

Whilst only approximate, the results presented here allow some conclusions of a general character to be drawn.

i. the distribution of radial displacement along the bearing is directly related to the pressure distribution;

ii. steep pressure gradients tend to generate tensile tangential stresses at the surface of the bearing due to localised bending;

iii. the stiffness of the backing has a strong influence on the magnitude of the tensile stresses that develop at the surface of the antifriction lining. Thence big-end connecting-rod bearings, particularly the bearing caps of the modern automotive engines, are more susceptible to fatigue failure de to the fact that they are generally less rigid than main crankshaft bearings and have to support the full loading from the ignition of the cylinders (Xu and Crooks, 1997);

iv. it can be seen that distinct meshes give rise to different values of the peak pressure p_{max} and different positions for the end of the pressure region. Although this latter difference is not significant when a fine mesh is used, the end position of the high pressure region can be markedly different if a coarse mesh is used .

5. Acknowledgements

.

6. References

ANSYS, 2002, Ansys Theory Reference, http://www1.ansys.com/customer/content/documentation/60/theorytoc.html http://www1.ansys.com/customer/content/documentation/60/ch11.html.

Bathe, K. J., 1996, Finite Element Procedures, Prentice-Hall.

Brebbia, C. A., 1987, Coupled Systems, Finite Element Handbook, edited by Kardestuncer, H., McGraw-Hill, New York, Part 3, Chapter 5, pp.3.285-3.287.

Boedo, S., 2002, Elastohydrodynamic Lubrication of Conformal Bearing Systems, ANSYS 2002 Conference Proceedings, Pittsburg, PA, USA.

Burnett, D. S., 1987, Finite Element Analysis from Concepts to Applications, Addison-Wesley.

Desai, C. S. and Abel, J. F., 1972, Introduction to the Finite Element Method A Numerical Method for Engineering Analysis, Van Nostrand Reinhold.

Joyce, M. R., 1999, Fatigue Failure of Automotive Bearings, Engineering Materials, University of Southampton, Southampton, UK. (Private communication.)

Melosh, R. J. and Utku, S., 1987, Principles for Design of Finite Element Meshes, Finite Element Handbook, edited by Kardestuncer, H., McGraw-Hill, New York, Part 3, Chapter 8, pp.3.425—3.440.

Shigley, J. E., 1972, Mechanical Engineering Design, second edition, McGraw- Hill.

Pinkus, O. and Sternlicht, B., 1961, Theory of Hydrodynamic Lubrication, McGraw- Hill, New York.

Villar, M. M., 2003 Elastic Analises of Fluid Film Bearings, M.Sc. dissertation, Faculdade de Engenharia Mecânica, Universidade Federal de Uberlândia, Uberlândia, Brazil.

White, F. M., 1991, Viscous Fluid Flow, second edition, McGraw-Hill.

www.math.ubc.ca/ feldman/m256/richard.pdf, 2001, Mathematics Department, University of British Columbia, Vancouver, Canada.

Xu, H., 1997, Elastohydrodynamic Lubrication in Plain Bearings, Elastohydrodynamics' 96, Tribology Series, 32, edited by D. Dowson et al., Elsevier Science B. V., pp.641—650. (Proceedings of the 23rd Leeds-Lyon Symposium on Tribology, held in the Institute of Tribology, Department of Mechanical Engineering, The University of Leeds, UK. 10th - 13th September, 1996.)

Xu, H. and Crooks, C. S., 1997, A Study of the Behaviour of Connecting Rod Bearings Using an EHL Predictive Tool, SAE Technical Paper Series, Paper no.970217, SAE International Congress & Exposition, Detroit, Michigan, February 24-27.

Zienkiewicz, O.C. and Taylor, R. L., 1991, The Finite Element Method – Solid and Fluid Mechanics, Dynamics and Non-Linearity, fourth edition, Vol.2, McGraw- Hill.